Increased layer interdiffusion in polyelectrolyte films upon annealing in water and aqueous salt solutions

ARTICLE *in* PHYSICAL CHEMISTRY CHEMICAL PHYSICS · JANUARY 2007

Impact Factor: 4.49 · DOI: 10.1039/b609440f · Source: PubMed

5 AUTHORS, INCLUDING:

Thomas Krebs
FMC Technologies Inc.
21 PUBLICATIONS **165** CITATIONS
SEE PROFILE

Gunther G Andersson
Flinders University
80 PUBLICATIONS **812** CITATIONS
SEE PROFILE

Harald Morgner
University of Leipzig
131 PUBLICATIONS **1,770** CITATIONS
SEE PROFILE

Increased layer interdiffusion in polyelectrolyte films upon annealing in water and aqueous salt solutions.
Thomas Krebs, Hazel L. Tan, Gunther Andersson, Harald Morgner and P. Gregory Van Patten
Phys. Chem. Chem. Phys., 2006, 8, 5462-5468
DOI: 10.1039/B609440F

Increased layer interdiffusion in polyelectrolyte films upon annealing in water and aqueous salt solutions

Thomas Krebs,*[a] Hazel L. Tan,[b] Gunther Andersson,[a] Harald Morgner[a] and P. Gregory Van Patten[b]

Received 4th July 2006, Accepted 23rd October 2006
First published as an Advance Article on the web 6th November 2006
DOI: 10.1039/b609440f

As-deposited films of multilayered polyelectrolytes are considered to be non-equilibrium structures. Due to the strong attraction between oppositely charged polyions, polyelectrolyte interdiffusion is thought to be suppressed during the adsorption process. Equilibration is promoted by a decrease of the electrostatic attraction between polyion pairs. We have used neutral impact collision ion scattering spectroscopy to investigate the influence of polyelectrolyte multilayer annealing in water and aqueous 1 M NaCl solutions at different temperatures (20 and 70 °C) on the increase in interpenetration of a single polyelectrolyte layer throughout the whole film. The multilayers were composed of poly(4-vinylpyridinium) and poly(4-styrenesulfonate). Contrast between neighboring layers was established by labelling the layer in question with the heavy atom ruthenium. It is found that both temperature and salt increase layer interpenetration, whereas salt has a stronger influence than temperature. From numerical simulations polyelectrolyte diffusion coefficients were evaluated for the different annealing conditions. The influence of temperature and salt on the equilibration of the film is interpreted in terms of increased screening of polyion charges and binding of small counterions to polyion monomeric units.

Introduction

The alternating adsorption of polyelectrolytes from aqueous solution on oppositely charged surfaces to obtain multilayered films was first reported by Decher *et al.*[1,2] Many fundamental aspects of polyelectrolyte multilayer formation and structure have been investigated until now. Examples are the influence of deposition conditions on film structure,[3–5] internal ordering and composition,[6,7] buildup mechanism[9,10] and response of the films to external conditions after deposition.[11–13]

Polyelectrolyte films are non-equilibrium structures with a kinetic hindrance to equilibrate due to the strong nature of the electrostatic attraction between oppositely charged polyions. In linearly growing systems, the polyions that are deposited during an adsorption step cannot diffuse into the entire film, but are bound by the last deposited oppositely charged layer. Interdiffusion is limited to a few neighboring layers.[6–8] If one assumes an Arrhenius-like relationship for the rate of interdiffusion, equilibration should be promoted by either a lowering of the energy barrier or an increase in temperature as has been suggested in ref. 5. The lowering of the energy barrier can be achieved by immersing the film into water or aqueous salt solutions to screen the opposite charges. Another effect of salt addition is that the salt ions compete with the polyelectrolyte ionic groups for binding sites. This competition can lead to dissociation of the polyelectrolyte ion pairs, and thus should increase the mobility of dissociated polyelectrolyte segments. In general, one would expect that the film is in thermodynamic equilibrium when no more irreversible layer interdiffusion takes place upon film exposition to any of the aforementioned conditions.

Very recently Jomaa *et al.* investigated with neutron reflectivity the interdiffusion of polyelectrolyte chains in poly(diallyldimethylammonium)/ poly(4-styrenesulfonate) (PDDA/PSS) multilayers upon exposure to aqueous salt solutions.[14] Deuterated PSS was used to obtain contrast between neighboring layers. They found that d-PSS diffused significantly into adjacent layers when immersing the film into a 0.8 M NaCl solution. They showed that polyelectrolyte interdiffusion takes place in the bulk of PEM upon exposition to salt solutions thus confirming the idea of polyelectrolyte multilayers being non-equilibrium structures.

Dubas *et al.*[15] and McAloney *et al.*[16] found a decrease in surface roughness of PDDA/PSS films upon immersion into aqueous solutions of NaCl. This decrease can be understood in terms of enhanced polyelectrolyte segment mobility. However one of the driving forces for reducing surface roughness in this case is probably the tendency to reduce the area between the solution and the hydrophobic film surface. Because this driving force is absent in bulk diffusion, a direct comparison between bulk and surface diffusion in PEM is difficult to achieve.

The aim of the present work is to investigate the influence of both temperature and salt on the magnitude of polyelectrolyte interdiffusion in PEM. In a previous paper we have shown the

[a] *University of Leipzig, Wilhelm-Ostwald-Institute of Physical and Theoretical Chemistry, Linnestrasse 2, 04103 Leipzig, Germany. E-mail: thomaskrebs@gmx.de; Fax: +49 341 9736090; Tel: +49 341 9736217*
[b] *Department of Chemistry and Biochemistry, Clippinger Laboratories, Ohio University, Athens, OH 45701-2979, USA. E-mail: vanpatte@ohio.edu; Fax: +01 740 593 0148; Tel: +01 740 517 8479*

applicability of neutral impact collision ion scattering spectroscopy (NICISS) for determining the degree of interpenetration between individual layers in PEM.[7] The depth distribution of polyelectrolyte chains from a single layer can be determined with NICISS by labeling the layer in question with a heavy atom such as ruthenium. The same labeling procedure was applied in the present study to determine the increase in spreading of a single layer over the entire film after the sample was subjected to different annealing conditions.

Experimental

Preparation of the PEM Films

Ruthenium was integrated into the polyelectrolyte films as $\{[(tpy)(bpy)Ru(PVP)(PVP)_x]^{2+}[(ClO_4)^-]_2\}_n$ (PVP = poly (4-vinylpyridine)). The compound was synthesized following a procedure that has been reported previously.[17] $RuCl_3 \cdot H_2O$ was purchased from Strem Chemicals. PDDACl (M = 400 000–500 000 g mol^{-1}), NaPSS (M = 70 000 g mol^{-1}), 2,2′-bipyridine and 2,2′:6′2″-terpyridine were purchased from Aldrich. PVP (M = 150 000–200 000 g mol^{-1}) was obtained from Polysciences Inc. Si-[100]-wafers were purchased from Virginia Semiconductor. All reagents were used without further purification.

All substrates were cleaned with piranha solution before deposition of the polyelectrolytes. Deionized water was used for the preparation of the solutions and the rinsing steps of the deposition procedure. The concentration of the PSS and PDDA solutions was 1 mM of monomeric units. The concentration of PVP was 10 mM of monomeric units. The Ru-PVP complex was dissolved in water to give a concentration of 85.7 mg per 100 mL. The pH of the PVP and Ru-PVP solutions was adjusted to 2.5 by adding HCl for the protonation of PVP to polyvinylpyridinium (PVPH). The ionic strength of the solutions was set to 0.1 M by adding NaCl. The films were prepared by alternately dipping the substrate into the polyelectrolyte solutions to yield 10 bilayers. The substrate was rinsed with deionized water after each deposition step. The deposition was carried out using a home built robot (LEGO RCX Invention System 2.0). All wafers were rotated at ~600 rpm during the deposition steps. Five samples were prepared in this way under the same deposition conditions.

The layer sequence is depicted in Scheme 1. Ru-PVP was deposited in the 8th bilayer, the numbering of the layers starts from the substrate.

Neutral impact collision ion scattering spectroscopy

Neutral impact collision ion scattering spectroscopy (NICISS) was used for the characterization of the Ru-labelled films. NICISS permits the determination of the elemental depth distribution in thin amorphous films. A comprehensive introduction to the basic principles of ion scattering is provided in ref. 18.

In NICISS experiments an ion beam is directed towards the sample. The ions are backscattered from the sample thereby losing energy. The energy loss consists of an elastic and an inelastic component. When the elastic energy loss is known, the mass of the target atom can be calculated from the laws of conservation of energy for collisions between two classical collision partners.[18]

The inelastic energy losses are caused by small-angle-scattering events and electronic excitations of the target atoms in the sample. The inelastic energy loss per depth interval is called stopping power. If the stopping power is known, the energy spectrum of the projectile can be converted to a depth profile.[19]

When using rare gas ions as projectiles nearly all of the projectiles leaving the sample are neutralized. For that reason the energy of the backscattered atoms is determined by measuring their time of flight.

He^+ was used as a projectile. The backscattering angle was 168°. The primary energy of the ion beam in our experiments was chosen to be 4.5 keV. At this energy depth profiles of ruthenium up to a depth of 25 nm can be determined reliably.

The sample was mounted on a steel disk. The steel disc was rotated and the distance between the centre of the sample and the position of the ion beam was changed periodically to avoid damaging of the sample. The chamber pressure ranged from 1×10^{-5} mbar to 5×10^{-5} mbar during the measurements.

A more detailed description of the principles of NICISS and the experimental setup used in this work can be found in ref. 20.

Treatment of the PEM films after preparation

The freshly prepared PEM films were subjected to NICISS measurements to determine the depth distribution of the Ru-labelled layers. After the measurements each of the five as-deposited films was subjected to a different annealing condition. The film was immersed for 60 min either in pure water or in 1 M NaCl solutions, at 20 °C or at 70 °C solution temperature. The annealed films were rinsed with pure water after the treatments. After annealing the samples were transferred to the vacuum chamber and NICIS spectra were measured again. An overview of the different treatment conditions is given in Table 1.

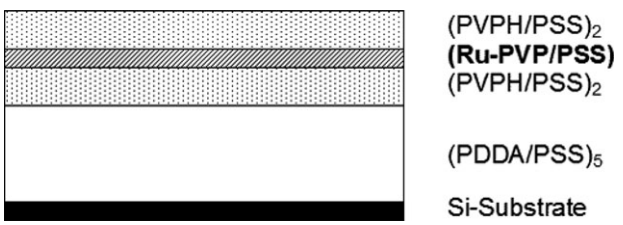

Scheme 1 Layer sequence of the PEM films.

Table 1 Summary of the different post-deposition treatment conditions

Sample	T/°C	c_{NaCl}/M
22_0	22	0
0_0	70	0
22_1	22	1
50_1	50	1
70_1	70	1

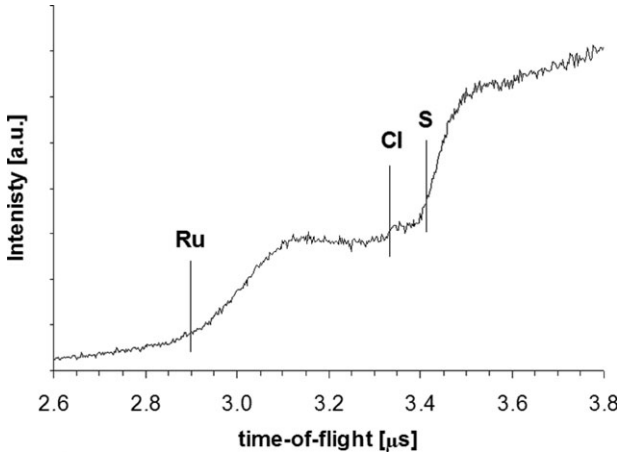

Fig. 1 NICIS spectrum of sample 70_0 before the post-deposition treatment, vertical lines indicate the onsets of the different elemental signals.

Results and discussion

Evaluation of Ru depth profiles before and after annealing

Fig. 1 shows the NICIS spectrum of sample 70_0 before it was annealed as an example in the time-of-flight region containing the ruthenium signal. The vertical lines indicate the onsets of the signals from the different elements. The signal starting at $\sim$2.95 μs and exhibiting a peak at $\sim$3.15 μs can be attributed to ruthenium, the small signal showing a peak at $\sim$3.35 μs to chloride and the step like signal with its onset at $\sim$3.40 μs to sulfur which is representative for the depth distribution of the PSS ions. These signals are superimposed onto a smooth background signal which is caused by sputtered hydrogen atoms.

Fig. 2a and 2b show the NICIS spectral regions with the Ru signals of all samples before and after annealing. The spectra are vertically offset for clarity.

The spectral position and shape of the chloride signal reveals that chloride is present only at the surface. A quantitative evaluation of that signal yields an average chlorine surface concentration of the order $(3 \times 10^{-11} \pm 2 \times 10^{-11})$ mol cm^{-2} for all the samples before and after the annealing treatments. This value was obtained assuming a sample density of 1 g cm^{-3} and an average molar mass of the film of 14 g cm^{-3}, which corresponds to the molar mass of a methylene unit. With these assumptions it is possible to determine a conversion factor between intensity and concentration by determining the height of the carbon step signal.[23]

For comparison, the counter ion surface charge density in the PDDA/PSS system found by us is of the order $\sim 2 \times 10^{-10}$ mol cm^{-2}.[21] Schlenoff *et al.* found a chloride surface density of the order $\sim 10^{-9}$ mol cm^{-2} using the radiotracer method for the same multilayer system.[22] Although the discrepancy between the results obtained with different methods cannot be explained, both values for the PDDA/PSS system are significantly larger than the chloride surface density in the PVPH/PSS system.

Due to the large error bars of the chlorine signal no reliable statements can be made about whether the chloride surface concentration might have changed upon exposing a sample to a certain post-deposition treatment. It has been shown for PDDA/PSS films that a fraction of the polyelectrolyte charge at and near the film surface is neutralized by small counter ions.[10] In the case of a PSS-terminated PVPH/PSS film one would expect this negative charge to be neutralized by sodium ions. However, no sodium signal could be found in the NICIS spectra. The upper limit for the sodium ion surface concentration considering the statistical error of the spectra can be evaluated to be $\sim 10^{-11}$ mol cm^{-2}. In conclusion, the charge compensation in the PVPH/PSS multilayer system between the two polyions is completely intrinsic in the bulk and mostly intrinsic also at the surface with a fraction of polycationic charges being neutralized by chloride ions. This result is in disagreement with the results obtained from radiotracer experiments by Schlenoff *et al.*[10] In contrast, a large amount of positive counter ions was found at the film surface when the films were capped with a PSS layer. The reason for this discrepancy is unknown.

The extraction of depth profiles from time-of-flight spectra has been described before.[7,23] Basically the procedure consists of fitting a polynomial to the background at times of flight higher and lower than the Ru signal. At higher times of flight the background superimposes with the sulfur signal. Because

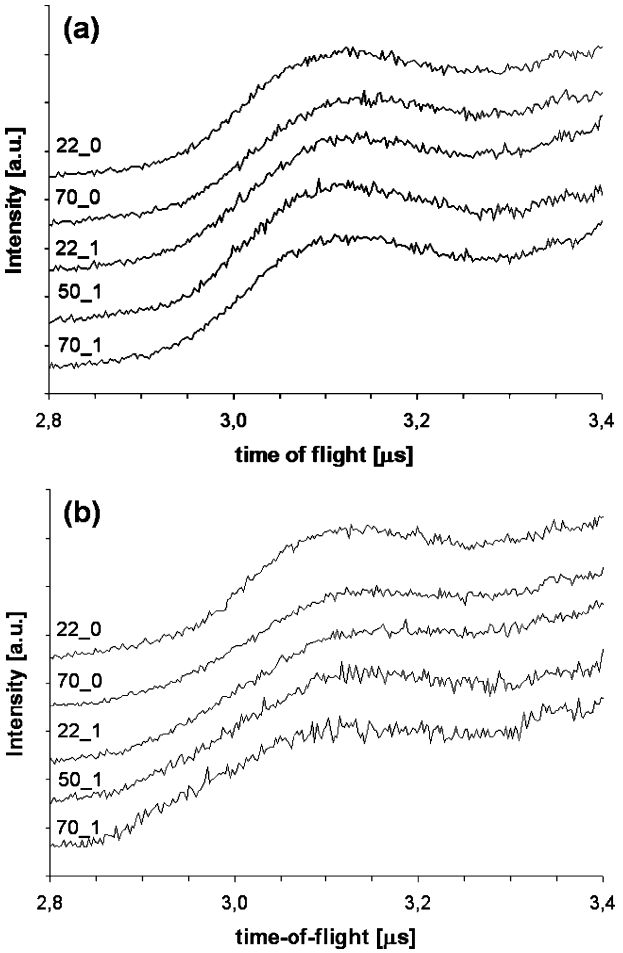

Fig. 2 NICIS spectra of all samples before (a) and after (b) annealing, spectra are vertically offset for clarity.

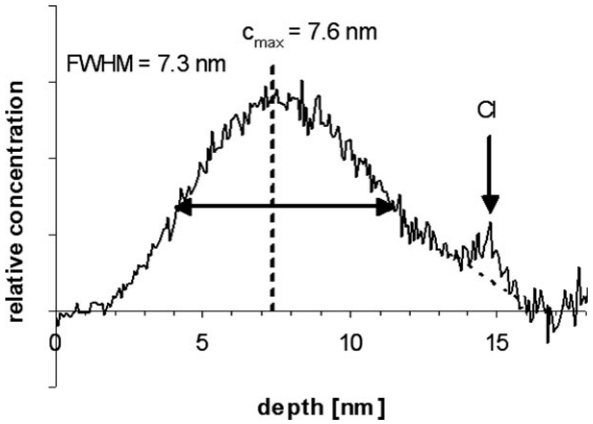

Fig. 3 Ru depth profile of sample 70_0 before the post-deposition treatment, the small peak labelled "Cl" denotes the chloride signal that is caused by chloride at the surface of the film, the dotted line shows a polynomial that was used to interpolate the chloride signal.

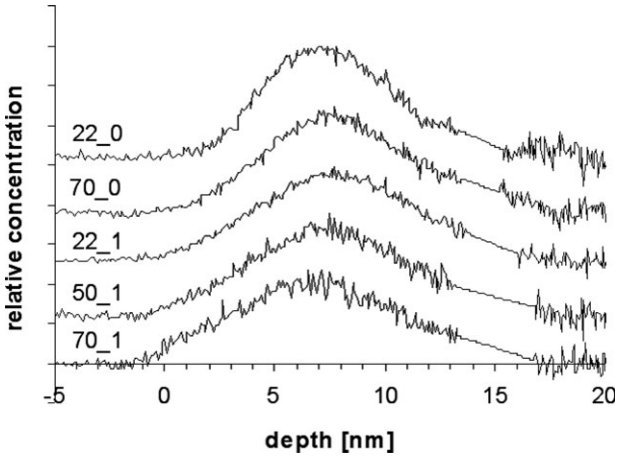

Fig. 4 Ru depth profiles of all samples after the annealing treatments; spectra are vertically offset, the different annealing conditions are indicated, the smooth curves in the depth interval of 13–17 nm are due to the removal of the chloride signal interfering with the Ru signal.

of the homogeneous bulk distribution the sulfur signal can be described by a step function. To account for limited experimental resolution the step function is convoluted with a Gaussian. The parameters of the Gaussian and the step height are determined from the spectrum of an unlabelled sample. Their values are chosen in such a way that the remaining background signal after subtraction of the sulfur signal yields a smooth curve. The same convoluted step function is also subtracted from the spectra of the labelled samples.

Fig. 3 shows the Ru depth profile of sample 70_0 before the post-deposition treatment. The small maximum at a depth of $\sim$14.5 nm is due to the chloride signal overlapping with the Ru signal. The signal is caused by chloride ions present at the surface of the film because the energy loss for chloride at the surface of the film is the same as for Ru in a depth of 14.5 nm. The dotted curve in the depth interval between 13.5 and 16.0 nm is due to the removal of the chloride signal being replaced by a fitted polynomial.

The Ru signal maximum is located at a depth of z_{max} = (7.6 $\pm$ 0.3) nm, the FWHM is (7.3 $\pm$ 0.2) nm. The average signal maximum of all five depth profiles is (7.2 $\pm$ 0.3) nm with a standard deviation of 0.3 nm. The average FWHM is (7.1 $\pm$ 0.2) nm with a standard deviation of 0.2 nm.

From the position of the signal maximum the average thickness of a PVPH/PSS bilayer can be estimated. Since we do not know the thickness increments for single PVPH or PSS layers, we shall assume that 2.5 bilayers are deposited on top of the Ru-PVP layer. From these considerations an average bilayer thickness of 2.9 nm is obtained. This result agrees with the value determined by ellipsometry in a previous study.[7] The FWHM indicates that Ru-PVP diffuses approximately halfway into each adjacent bilayer which also agrees with the result from ref. 7. All these results underscore the good reproducibility of PEM film preparation.

Fig. 4 shows the Ru depth profiles of all samples after they were subjected to different annealing conditions. The curves are vertically offset for clarity. Since the depth scales for ruthenium and chloride are different, all chloride signals were replaced by fitted polynomials.

As can already be seen from a visual inspection of the depth profiles, the spread of the labelled layer is largest for the samples that have been annealed in salt solutions and at elevated temperatures. The increased spreading of the labelled layer over the whole film for the different samples can be quantified. Table 2 lists the differences $\Delta\delta$ between the FWHM of the different samples before and after the annealing.

One possible error source is not included in the error bars in Table 2. As already noted it has been found that immersion of PEM into salt solutions reduces the surface roughness of the films. A change in surface roughness can influence the resolution of NICISS. The consequences of this process for the results presented above shall be discussed in the following.

NICISS probes the amount of matter along the z-axis between the surface and a target atom within the film. A surface roughness value that is different from zero can cause a distribution of lengths the helium ions have to pass before collision. This leads to a broadening of the signal from the labelled layer on the energy or depth scale.

More generally speaking the actual depth profile $c(z)$ is convoluted with a surface roughness distribution $r(z)$ to yield the apparent depth profile $c'(z)$ according to:

$$c'(z) = \int_{-\infty}^{\infty} r(z - z')c(z')\,\mathrm{d}z' \qquad (1)$$

A smoothing of the surface upon annealing will lead to a narrowing of the length distribution $r(z)$, assuming that the surface diffusion occurs much faster than bulk diffusion which

Table 2 Increase in FWHM of the labelled layers $\Delta\delta$, obtained for the different annealing and the diffusion coefficient obtained from the simulations using eqn (2)

Sample	$\Delta\delta$/nm	$D/10^{-4}$ nm^2 s^{-1}
22_0	0.1 $\pm$ 0.02	2 $\pm$ 1
70_0	0.7 $\pm$ 0.2	5 $\pm$ 2
22_1	1.1 $\pm$ 0.3	5 $\pm$ 2
50_1	1.7 $\pm$ 0.3	5 $\pm$ 2
70_1	2.4 $\pm$ 0.3	15 $\pm$ 3

has been shown for the PDDA/PSS system.[14,15] AFM measurements have not been performed after annealing of the samples so the change in root mean square (rms) surface roughness, respectively the surface roughness distribution cannot be determined. The actual depth profiles may be broader than the measured signals due to a decrease in surface roughness. For that reason the $\Delta\delta$ values shown in Table 2 can be taken as a lower limit for polyelectrolyte interdiffusion. The decrease in surface roughness also becomes larger with increasing temperature and salt concentration. This means that the qualitative behavior of the $\Delta\delta$ dependence on temperature and salt concentration will not change. However, a full quantitative evaluation is not possible.

The rms surface roughness of PVPH/PSS films before annealing is of the order of 3.5 nm.[7] This value sets the upper limit for the error bars of $\Delta\delta$. However there is reason to assume that the actual error is much lower than 3.5 nm. It has been suggested that the rate of surface diffusion—and hence the rate of surface smoothing—should depend on the counter ion concentration at and near the film surface.[14] A smaller number of polyion pairs would need to dissociate if a fraction of polyions binds to small counter ions. Consequently the polyelectrolyte mobility will be larger if small counter ion are present at the surface. Since the counter ion concentration at the surface of the PVPH/PSS films is very small, surface diffusion should proceed much slower than in the PDDA/PSS system.

Estimation of polyelectrolyte diffusion coefficients from diffusion simulations

From the increased spread of the Ru-labelled layers polyelectrolyte diffusion coefficients for the different annealing conditions can be obtained. Numerical diffusion simulations were carried out using custom C code written by the authors for this purpose. The simulation is based on Fick's first law:

$$J(z) = -D\left(\frac{\partial c}{\partial z}\right) \qquad (2)$$

where J is the net flux (mol nm^{-2} s^{-1}) of material in the z direction through an imaginary interface located at depth z, D is the diffusion coefficient (nm^2 s^{-1}), and c is the concentration at depth z. This model should be justified since one would expect the equilibrium situation of the film to be a spatially homogeneous distribution of all components.

The pre-anneal ($t = 0$) depth profiles were used to calculate the concentration gradient ($\mathrm{d}c/\mathrm{d}z$) as a function of depth. The net flux was then calculated using eqn (2) and multiplied by an infinitesimal time interval, $\mathrm{d}t$ to compute the net amount of material, $\mathrm{d}N$, traversing the interface in the z direction within the time interval $\mathrm{d}t$. This quantity, $\mathrm{d}N$, was then added to the initial concentration profile at the position ($z + \mathrm{d}z$) to generate the concentration profile at time $\mathrm{d}t$. The process was then repeated using the profile obtained for $t = \mathrm{d}t$ in order to compute the depth concentration profile at $t = 2\ \mathrm{d}t$, and so on until the final concentration profile was obtained for $t = 3600$ s. The interval $\mathrm{d}t$ was varied in the simulations from 0.005 to 0.1 s to ensure that the choice of $\mathrm{d}t$ did not affect the result. The diffusion coefficient was varied in order to find the value which gave the closest agreement with experiment. No initial smoothing of the pre-anneal depth profiles was performed.

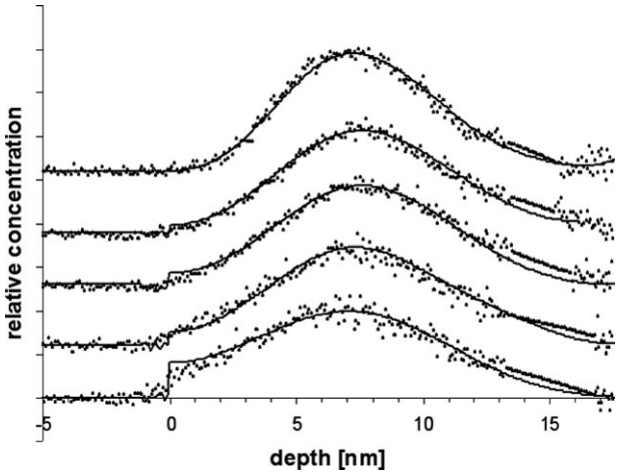

Fig. 5 Fitted curves (solid lines) to the Ru depth profiles after annealing (small circles) using eqn (2).

Fig. 5 shows the best fits to the Ru depth profiles after annealing obtained using the simulations. In Table 2 the diffusion coefficients obtained from the simulations for the different annealing conditions are listed.

Discussion

As can be seen from the increase in FWHM of the Ru signals (Table 2), both temperature and salt give rise to an increased interdiffusion of the polyelectrolyte chains in the film. Even the immersion of the film into pure water at room temperature causes a small but measurable increase of polyelectrolyte segment interpenetration. These results support the idea of polyelectrolyte multilayer films being non-equilibrium structures.

The observation that the immersion into pure water at room temperature already leads to an increased layer interpenetration can be understood in terms of an increased screening of polyion charges due to the immersion of the film into a solvent with high dielectric constant. As a consequence the probability for dissociation of individual polyion pairs increases thus leading to a larger mobility of polyelectrolyte segments.

However the increase in layer interpenetration upon immersion of the film into water at 22 °C is small compared to the treatment in water at 70 °C. An increased thermal energy of the polyions at 70 °C facilitates an overcoming of the electrostatic attraction between oppositely charged segments.

Salt has an even stronger effect on layer interdiffusion than temperature when comparing the increase in FWHM of 0.7 nm upon film immersion in 70 °C water and 1.1 nm upon immersion in 1 M NaCl aqueous solution at 22 °C.

In the framework of treating the solvent as a dielectric continuum, salt addition changes the macroscopic dielectric constant, without degrading the homogeneity of the solvent. The macroscopic dielectric constant of a 1 M NaCl aqueous solution is 14% lower than that of pure water.[24] Electrostatic screening in a 1 M NaCl solution therefore would be even

smaller than in pure water and thus such a large increase in layer interpenetration is not expected.

However, as already noted, the inorganic salt ions can have a strong local effect on the screening between two oppositely charged polyions. Exposure of the film to a solution containing small counter ions can be imagined to lead to a competition of binding sites between the polyions and the small counter ions. This ion exchange can be expressed as the following equilibrium:[10]

$$P^+P^- + C^+ + C^- \rightleftharpoons P^+C^- + C^+P^- \qquad (3)$$

P^+ and P^- denote the positive and negative polyions. C^+ and C^- denote the small counter ions. The binding of small counter ions to the polyions increases the mobility of polyelectrolyte segments thus facilitating interdiffusion within the film. From the considerations about the effect of salt upon layer interdiffusion it seems likely that the increase of polyelectrolyte mobility is mainly caused by the binding of small counter ions to individual polyion monomeric units.

It is not surprising that layer interdiffusion becomes even stronger when exposing the film to salt solutions at elevated temperatures. Unfortunately due to the unknown error associated with the probable decrease of the surface roughness as already discussed, a quantitative relationship between increase in FWHM of the Ru signal and temperature cannot be obtained.

The trend in the diffusion coefficients obtained from the simulations follows the trend in the broadening of the Ru signals obtained for the different annealing conditions. Jomaa *et al*. determined a diffusion coefficient from the spread of a deuterated PSS-layer over the film as a function of time.[14] They found a value of the order 2×10^{-3}–6×10^{-3} $nm^2\ s^{-1}$ when exposing a PDDA/PSS film to a 0.8 M NaCl solution at room temperature. This value is approximately one order of magnitude larger than the diffusion coefficient of 5×10^{-4} $nm^2\ s^{-1}$ found by us for treatment conditions of 1 M NaCl and room temperature. The most probable explanation for this discrepancy are the differences between the polymer systems under study. Unlike PDDA, the Ru-PVP polycation studied here is divalent, so the Coulombic attraction between Ru-PVP and PSS is larger than that of the PDDA/PSS system. Moreover, two counter ions are required to render each Ru-PVP unit mobile. In addition to these electrostatic effects, the Ru-PVP monomers are considerably bulkier than the PDDA units. Together, these two effects may considerably lower the diffusion coefficient in this system compared with the PDDA/PSS system.

The labelling scheme used in this work relies on the introduction of a probe element (Ru in this case) to the system. In general, such a practice alters the chemistry of the system and may actually affect the process under observation. In some cases, the chemical differences of the labelled system may limit the ability to draw conclusions about un-labelled systems of interest. For example, as mentioned above, the diffusion of the labelled polymer is approximately one order of magnitude slower than has been observed in a system containing PDDA as the polycation. While the magnitude of the diffusion rates in the present system varies from the more commonly used PDDA/PSS system, the trends reported here can be understood in terms of physical principles that are generally applicable to a wide variety of polycations, including PDDA. NICISS and elemental labelling appear to be well suited for such studies.

Conclusions

We have studied the magnitude of layer interdiffusion in polyelectrolyte multilayers upon annealing of the films in water and 1 M NaCl aqueous solutions at different temperatures. Neutral impact collision ion scattering spectroscopy was used to establish the concentration depth profile of a single layer in the film before and after the post-deposition treatments. To obtain contrast between neighboring layers the heavy atom ruthenium was used as a labelling agent. It was found that the diffusion of labelled chains upon annealing increases with temperature and is larger in NaCl solution than in water. These results reveal the non-equilibrium nature of as-deposited polyelectrolyte films. The finding that salt has stronger influence on chain mobility than temperature supports the idea that small counter ions compete with polyions for binding sites. This disentanglement of polyelectrolyte segments leads to an increase in polyelectrolyte chain mobility. Numerical simulations based on Fick's first law of diffusion were carried out to determine polyelectrolyte chain diffusion coefficients.

It was also found that the charge compensation in PVPH/PSS multilayers is completely intrinsic in the bulk and only weakly extrinsic at the surface of the film.

The influence of a possible change in surface roughness during the annealing on the resolution of the method was discussed. It was asserted that a change in surface roughness leads to an underestimation of the polyelectrolyte diffusion in the film during the post-deposition treatment.

Acknowledgements

The authors are grateful for financial support provided by the International Postgraduate Programme of the University of Leipzig and the Internationale Studien- und Ausbildungs partnerschaften Programme of the DAAD. Funding support from the Ohio–Leipzig Exchange Program is also gratefully acknowledged.

References

1 G. Decher and J. D. Hong, *Ber. Bunsen-Ges. Phys. Chem.*, 1991, **95**, 1430.
2 G. Decher, *Science*, 1997, **277**, 1232.
3 G. Decher, J. D. Hong and J. Schmitt, *Thin Solid Films*, 1992, **210**, 831.
4 E. Poptoshev, B. Schoeler and F. Caruso, *Langmuir*, 2004, **20**, 829.
5 H. L. Tan, M. J. McMurdo, G. Pan and P. G. Van Patten, *Langmuir*, 2003, **19**, 9311.
6 M. Loesche, J. Schmitt, G. Decher, W. G. Bouwman and K. Kjaer, *Macromolecules*, 1998, **8893**, 31.
7 H. L. Tan, T. Krebs, G. G. Andersson, D. Neff, M. Norton, H. Morgner and P. G. Van Patten, *Langmuir*, 2005, **21**, 2598.
8 J. W. Baur, M. F. Rubner, J. R. Reynolds and S. Kim, *Langmuir*, 1999, **15**, 6460.
9 K. Lowack and C. Helm, *Macromolecules*, 1998, **823**, 31.
10 J. B. Schlenoff, H. Ly and M. Li, *J. Am. Chem. Soc.*, 1998, **120**, 7626.

11 J. E. Wong, F. Rehfeldt, P. Haenni, M. Tanaka M and R. von Klitzing, *Macromolecules*, 2004, **37**, 7285.
12 G. B. Sukhorukov, J. Schmitt and G. Decher, *Ber. Bunsen-Ges. Phys. Chem.*, 1996, **100**, 948.
13 J. Ruths, F. Essler, G. Decher and H. Riegler, *Langmuir*, 2000, **16**, 8871.
14 H. W. Jomaa and J. B. Schlenoff, *Macromolecules*, 2005, **38**, 8473.
15 S. T. Dubas and J. B. Schlenoff, *Langmuir*, 2001, **17**, 7725.
16 R. A. McAloney, V. Dudnik and C. M. Goh, *Langmuir*, 2003, **19**, 3947.
17 J. M. Calvert and T. J. Meyer, *Inorg. Chem.*, 1981, **20**, 27.
18 D. Briggs and M. P. Seah, *Practical Surface Analysis, Vol. 2, Ion and Neutral Spectroscopy*, Wiley, New York, 1992.
19 G. G. Andersson and H. Morgner, *Nucl. Instrum. Methods Phys. Res., Sect. B*, 1999, **155**, 357.
20 G. G. Andersson and H. Morgner, *Surf. Sci.*, 1998, **405**, 138.
21 T. Krebs, G. G. Andersson, H. Morgner and P. G. Van Patten, unpublished work.
22 J. B. Schlenoff and S. T. Dubas, *Macromolecules*, 2001, **34**, 592.
23 G. G. Andersson, T. Krebs and H. Morgner, *Phys. Chem. Chem. Phys.*, 2005, **7**, 136.
24 J. B. Hasted, D. M. Ritson and C. H. Collie, *J. Chem. Phys.*, 1948, **16**, 1.

